Controlling Hydrogen Activation, Spillover, and Desorption with Pd-Au Single Atom Alloys

*Felicia R. Lucci[1], Matthew T. Darby[3], Michael F. G. Mattera[1], Christopher J. Ivimey[1], Andrew J. Therrien[1], Angelos Michaelides[2], Michail Stamatakis[3] and E. Charles H. Sykes[1]**

1 Department of Chemistry, Tufts University, 62 Talbot Avenue, Medford, Massachusetts 02155, United States
2 Thomas Young Centre, London Centre for Nanotechnology and Department of Chemistry, University College London, 17-19 Gordon Street, London, WC1H 0AH, UK
3 Thomas Young Centre and Department of Chemical Engineering, University College London, Roberts Building, Torrington Place, London, WC1E 7JE, UK

Author Information

Corresponding Author

*E-mail: charles.sykes@tufts.edu

Abstract

Key descriptors in hydrogenation catalysis are the nature of the active sites for H_2 activation and the adsorption strength of H atoms to the surface. Using an atomically resolved model system of dilute Pd-Au surface alloys and density functional theory calculations, we determine key aspects of H_2 activation, diffusion, and desorption. Pd monomers in a Au(111) surface catalyze the dissociative adsorption of H_2 at temperatures as low as 85 K, a process previously expected to require contiguous Pd sites. H atoms preside at the Pd sites and desorb at temperatures significantly lower than from pure Pd (175 versus 310 K). This facile H_2 activation and weak adsorption of H atom intermediates are key requirements for active and selective hydrogenations. We also demonstrate weak adsorption of CO, a common catalyst poison, forces H atoms to spillover from Pd to Au sites as evidenced by low temperature H_2 desorption.

TOC:

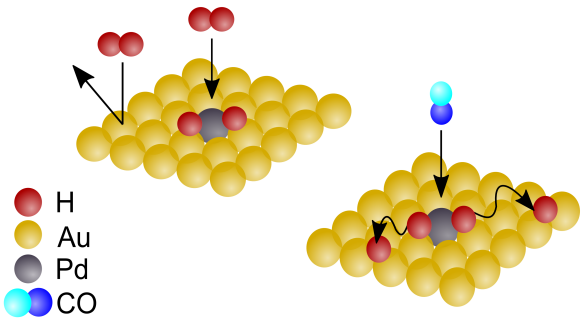

Keywords

Bimetallic alloys, temperature programmed desorption, scanning tunneling microscopy, density functional theory, hydrogenation

A key requirement in the efficient use of heterogeneous catalysts, fuel cells and hydrogen storage devices is the ability to activate, uptake and release hydrogen easily.[1–3] Metallic surfaces that bind H weakly can exhibit high catalytic selectivity; however, these surfaces often have high activation barriers for H_2 dissociation which limits the activity of the catalysts.[4,5] One viable approach to produce weakly bound H atoms on the surface of catalysts is to use a bimetallic alloy that combines reactive catalytic metals with inert coinage metals.[6–9] This alloy combination includes a catalytic metal that exhibits facile H_2 dissociation and a coinage metal that can utilize the weakly bound H atoms to catalyze hydrogenation reactions.[10–14]

Au nanoparticles have been recently shown to catalyze highly selective hydrogenation and oxidation reactions due to the weak adsorption energy of H and O on Au.[15–18] The addition of Pd into Au changes the catalytic activity and selectivity for multiple reactions including vinyl acetate synthesis,[19] hydrogen peroxide synthesis,[20] hydrocarbon hydrogenation,[21,22] CO oxidation,[23] and oxidation of alcohols to aldehydes.[24] For many of these reactions, the size and dispersion of the Pd atom clusters have an impact on the observed chemistry; the so-called ensemble effect in alloy catalysis.[25,26] Selective synthesis of vinyl acetate[19,27] and hydrogen peroxide[20] rely on the inability of Pd monomers to activate O_2 while CO oxidation requires Pd dimers to dissociate O_2.[23] For H_2 activation on Pd-Au, the necessary ensemble size has been debated. Yu *et al.* and Maroun *et al.* concluded that contiguous Pd atoms are required for H_2 activation.[28,29] But, density functional theory (DFT) calculations by Venkatachalam *et al.* indicated that Pd monomers may be capable of H_2 activation.[30] However, so far no experimental evidence exists demonstrating this single atom chemistry. Furthermore, CO is a common poison for catalysts. An understanding of CO interaction with adsorbed molecules and competition for actives sites is important when designing new catalysts. Hence, an atomic level understanding of

reactive sites for CO adsorption and H_2 activation will elucidate the minimal Pd ensemble capable of activating H_2 and reveal the energetic landscape for uptake, spillover and release of H and CO.

To probe the ability of Pd monomers in Au to activate H_2 and to induce spillover of H atoms onto Au, we studied the fundamental processes of dissociation, spillover, and desorption using the complementary techniques of scanning tunneling microscopy (STM), temperature programmed desorption (TPD) and density functional theory (DFT). STM enables direct visualization of the atomic composition of the active sites necessary for H_2 activation and TPD allows us to elucidate key parts of the energy landscape for activation, spillover and desorption. By studying dilute concentrations of Pd atoms (≤5%) in Au, we observe facile dissociation and low temperature recombinative desorption of H_2 from isolated Pd atoms in Au(111). Our Pd-Au single atom alloy (SAA) data contrasts with previous studies that suggested at least two contiguous Pd atoms are required for H_2 dissociation,[28,29] although this previous work lacked an atomic scale characterization of the alloy surface. Furthermore, we have discovered that the co-adsorption of CO with H forces H to spill over from the active Pd sites to Au. By comparing H_2 and CO desorption temperatures to calculated adsorption energies of H and CO, we elucidate the energetic pathway for the adsorption, spillover, and desorption of H with and without CO from Pd monomers in Au.

In order to determine if Pd monomers in Au are capable of H_2 activation, we first generated Pd-Au(111) alloys with isolated Pd atoms present in the surface layer (Figure 1). Pd-Au(111) alloys formed by the vapor deposition of Pd on Au(111) have been extensively characterized.[29,31–35] Depending on the surface temperature and flux of incoming Pd atoms during alloying, a range of structures can be formed from isolated atoms substituted into the

surface and subsurface layers of Au to Pd rich nanoparticles on the surface.[31–33] At low Pd coverages (≤0.05 ML), Pd atoms exists as isolated atoms substituted into the Au lattice. Due to stronger heteroatom bonds, Pd atoms prefer to be surrounded by Au atoms and exist as isolated species at low coverages.[30,36,37] At Pd coverages >0.05 ML, the Pd atoms begin to cluster due to a kinetic limitation on the dispersion of the Pd atoms in Au.[31] In the present study, all Pd-Au(111) alloys were prepared at 380 K yielding an alloyed surface where Pd atoms predominately exist as monomers in the Au surface at coverages below 0.05 ML.

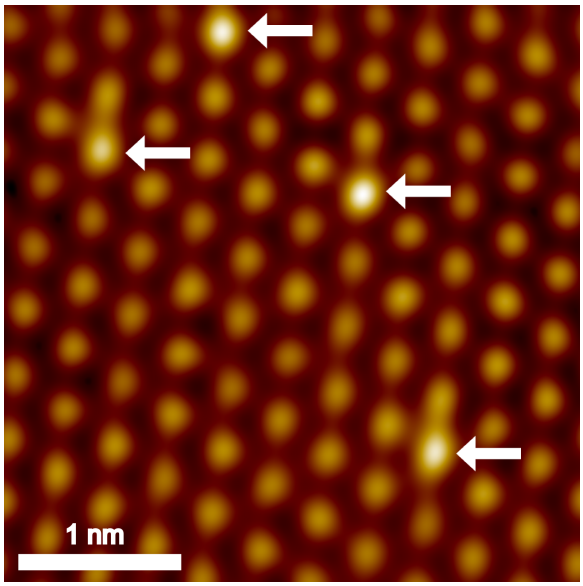

Figure 1. Pd-Au(111) SAA. Isolated Pd atoms (highlighted by arrows) substituted into Au(111) appear topographically higher than the Au host.

Using TPD, we investigated the ability of isolated Pd atoms to dissociate H_2 (Figure 2). We prepared Pd-Au(111) SAA with between 0.01 and 0.05 ML Pd and exposed them to H_2 at 85 K and observed the desorption of H_2 at 110 K and 175 K (Figure 2A). The predominant desorption peak at 175 K is due to H_2 desorption from single Pd atoms because increasing the Pd coverage leads to a linear increase in the area of the peak. In the absence of Pd atoms, no desorption of H_2 is observed from bare Au(111) after the same exposure to H_2. The desorption

temperature of H_2 at 175 K indicates H_2 dissociates on the surface since molecular H_2 desorbs from metal surfaces at <30 K.[38,39] Furthermore, our data shows that the desorption of H_2 from Pd monomers is significantly lower than the desorption of H_2 from Pd(111) which occurs at 310 K.[40] The small desorption peak seen in Figure 2A at 110 K is due to desorption of H_2 from Au sites as previously reported by Pan *et al.* who adsorbed H atoms onto Au(111) using a H atom source in order to overcome the dissociation barrier.[41] Additionally, in order to determine the desorption order of H_2, we varied the surface coverage of H. With increasing H coverage, the desorption peaks shift to lower temperatures indicative of second order desorption as previously observed for disordered Pd-Au alloys.[28]

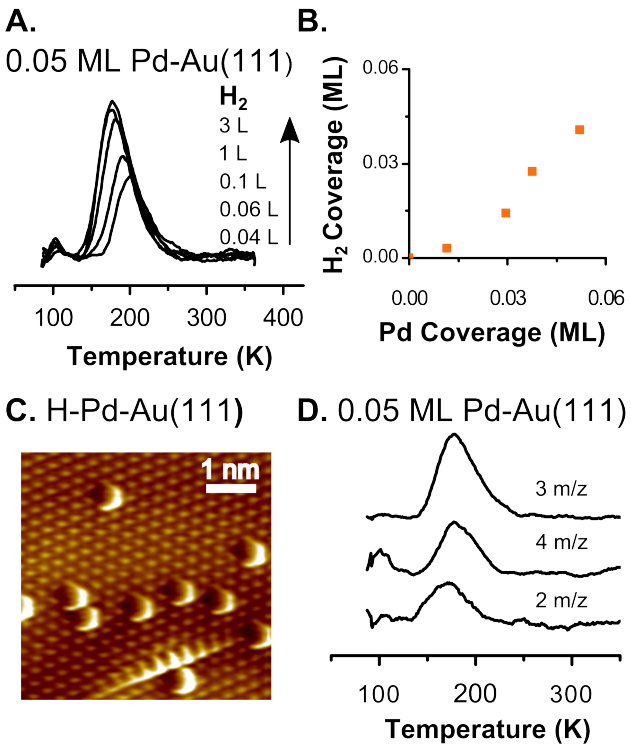

Figure 2. H_2 activation on Pd-Au SAAs. (A) TPD spectra of H_2 desorption from a 0.05 ML Pd-Au(111) SAA after exposure to H_2 at 85 K. (B) H_2 coverage on varying concentrations of Pd in the SAA regime. (C) STM image of Pd-Au(111) SAA exposed to H_2 and cooled to 5 K for imaging at -1 V and 1 nA. (D) Desorption traces for m/z 2, 3, and 4 from Pd-Au SAA with equivalent H_2 and D_2 coverages.

Figure 2B shows that in the single atom regime (<0.05 ML), the amount of H_2 desorbing from the surface is proportional to the amount of Pd atoms present in the surface with an average of 1.4 ± 0.1 H atoms per Pd atom. One to three H atoms are predicted by DFT to be thermodynamically stable in the three-fold hollow sites surrounding Pd monomers in Au.[30] Small amounts of H atoms spill over from the Pd sites to Au, but we are unable to quantify the amount of H_2 desorbing from Au since H_2 begins desorbing at the start of the temperature ramp. With STM we imaged Pd-Au(111) SAA exposed to H_2 and observed localized protrusions in the vicinity of edge-dislocations where Pd atoms predominately reside (Figure 2C). In accord with our TPD results, we suggest the enlarged appearance of the Pd atoms is due to the presence of H atoms at the Pd monomer sites. DFT and STM experiments support the suggestion that H atoms are thermodynamically stable on Pd-Au alloys.[30,42,43]

To further probe the H_2 activation and H atom mobility on Pd-Au SAAs we co-adsorbed H_2 and D_2 onto Pd-Au SAA (Figure 2D). When H_2 and D_2 were deposited on the SAA, we observed the desorption of H-D (m/z = 3). This scrambling provides direct evidence that Pd-Au SAAs are indeed capable of H_2 activation at 85 K. Furthermore, when equal amounts of H_2 and D_2 were activated, the H_2:HD:D_2 product ratio was 1:2:1 demonstrating complete scrambling of H and D. As evidenced by the small desorption peak at 110 K, the majority of the H_2 or D_2 does not desorb from the Au sites due to the larger desorption barrier from Au (0.69 eV). However, H can diffuse from one Pd atom to another Pd atom by overcoming the lower diffusion barrier onto the Au surface. On Au, H and D move very quickly due to the small diffusion barrier on Au of ~ 0.07 eV.[44] If H atoms were not able to diffuse across the Au surface, we would not have observed the complete statistical scrambling of H and D.

As a second probe of the surface chemistry of Pd-Au SAAs, we studied the adsorption of CO, a common catalyst poison. Figure 3 shows that after exposure of a Pd-Au SAA to CO, a CO desorption peak is observed at 270 K corresponding to an adsorption energy of - 0.7 eV assuming a pre-exponential factor of 10^{13} which reasonably compares to DFT calculated adsorption energy of -1.34 eV. This is a significantly lower desorption temperature than observed from pure Pd(111) (>450 K).[45] CO is also seen to desorb from Au terraces at <170 K and Au step edges at 180 K.[46] Low temperature desorption of CO from Pd-Au alloys has been reported for isolated Pd atoms in Au-Pd(111)[32] and Au-Pd-Mo(110).[47] Ruff *et al.* reported that the low desorption temperature of CO from Pd-Au alloys is due to the size of the Pd ensembles in Au.[32] Larger Pd ensembles increase the adsorption energy of CO to the surface. The weak adsorption of CO to Pd-Au SAAs that we observe is important for both catalyst and fuel cells applications in which active site poisoning by CO can be a serious issue.

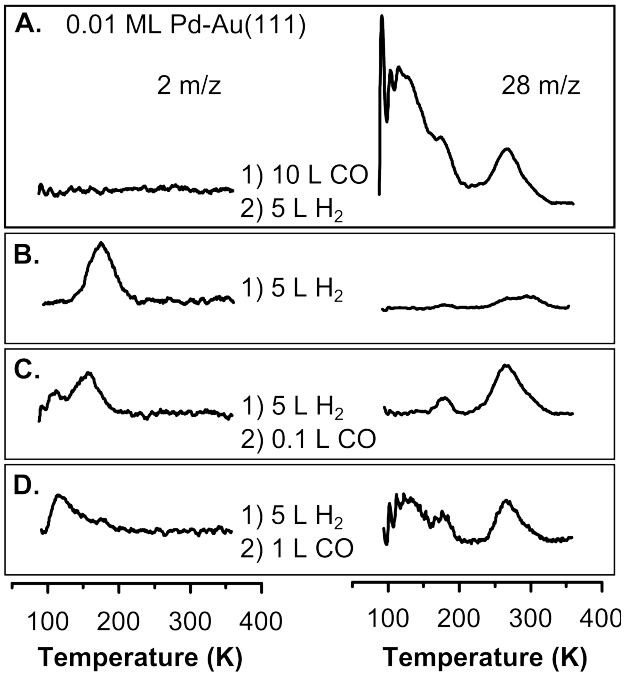

Figure 3. TPD traces for H_2 (left, 2 m/z) and CO (right, 28 m/z) desorption from Pd-Au SAA surfaces exposed to varying amounts of H_2 and CO. In panel A, 10 L CO is adsorbed and then 5 L H_2. In panel B, 5 L H_2 is exclusively adsorbed. In panel C, 5 L H_2 is adsorbed and then 0.1 L CO. In panel D, 5 L H_2 is adsorbed and then 1 L CO.

We discovered that CO can enhance the spillover of H atoms from Pd sites where H_2 predominantly desorbs from Au. Figure 3 shows TPD traces for the co-adsorption of H and CO where the desorption temperature of H_2 is dependent on the CO exposure. In the absence of CO, H_2 desorbs from Pd sites at 175 K (Figure 3B). At sub-saturation coverages of CO (0.1 L CO), we observed desorption of H_2 from both Pd (160 K) and Au (110 K) sites (Figure 3C). When the surface was exposed to 5 L H_2 followed by 1 L CO, all H_2 desorbs from the surface at 110 K since all the Pd atoms are saturated with CO (Figure 3D). Thus, it appears that when CO adsorbs on a H covered SAA surface, CO forces the H atoms on to the Au(111) terraces from where they desorb at a significantly lower temperature than otherwise observed in the absence of CO.

To further understand this desorption behavior, periodic DFT calculations were performed on unreconstructed Au(111) surfaces with the VASP 5.3.3[48,49] code employing the optB86b-vdW[50,51] exchange-correlation functional, which accounts for dispersion forces within the vdW-DF scheme of Dion et al[52] (see the Supporting Information for more details of the computational setup and energy definitions). In our DFT calculations a variety of CO, H and CO plus H adsorption structures were considered. With regard to the observed tendency of CO to drive H atoms away from the Pd sites of the SAA, our DFT calculations show that there is a strong repulsion between adsorbed CO and H. Specifically, when CO is adsorbed on the atop Pd site and H is in one of the adjacent three-fold hollow sites that surround the Pd atom there is a *ca.* 0.56 eV repulsion between CO and H (Table S3). This repulsion can be reduced to only 0.01 -

0.02 eV if the H atom moves away to a proximal hollow site surrounded by only surface Au atoms. Therefore, despite H atom spillover being unfavorable, when CO adsorbs to the Pd sites, it becomes favorable for H to move onto Au(111). Furthermore, if CO is adsorbed on the surface prior to H_2, no H_2 is observed desorbing from the surface. Therefore, CO binds to the Pd sites and blocks the adsorption and activation of H_2 which further supports our hypothesis that Pd atoms are the sites responsible for H_2 activation (Figure 3A). For a CO covered Pd(111), it has previously been shown that CO blocks the dissociative adsorption of H_2.[53] Related to these results, previous studies have demonstrated that the adsorption of CO on bimetallic alloys alters the desorption behavior of H_2. For $Pd_{70}Au_{30}$(110) alloys, the co-adsorption of CO and H increases the desorption temperature of H due to a trapping of near surface H.[54] A similar effect was observed for Pd-Cu alloys where CO selectively binds to the single Pd atoms in Cu and blocks the Pd entrance and exit sites for H_2 adsorption.[55] These mechanisms, called the *molecular cork effect,* allow H atoms to remain on the surface beyond their normal desorption temperature. Additionally, for Co nanoparticles supported on Cu(111), CO forces the spillover of H from Co to Cu sites via two-dimensional pressure.[56,57] However, the co-adsorption of CO on Pd-Au SAAs investigated in this study changes the H_2 desorption site. CO adsorption forces the H from the Pd sites to Au where it is weakly bound and it desorbs at 110 K; therefore, addition of CO alters the exit site for H_2 as shown in Figure 4.

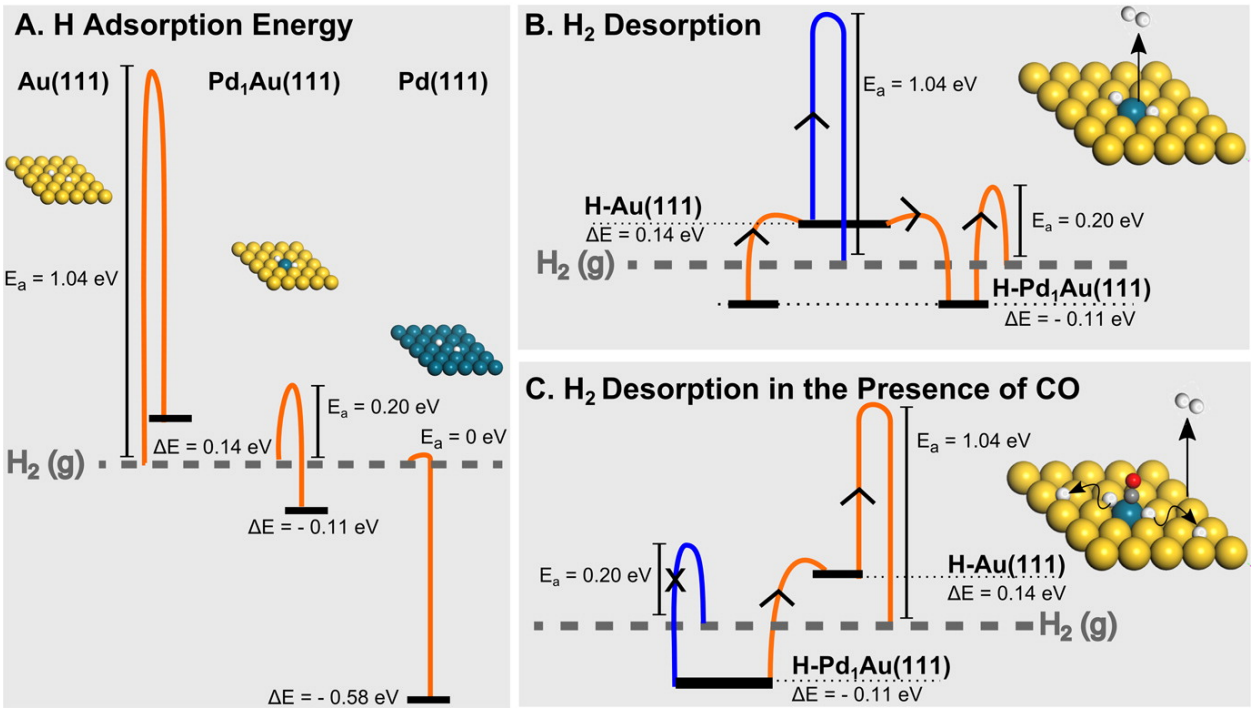

Figure 4. Schematics of the energy landscapes for H_2 adsorption and desorption. (A) H_2 activation energy (E_a),[5,58] energy of transition state (E_T) and H adsorption energy (ΔE) per H atom on monometallic Au, Pd and Pd-Au SAA. Energetics of H_2 desorption for Pd-Au SAA (B) without and (C) with CO. Schematic illustrates the preferred active sites for H_2 dissociation as well as preferred adsorption sites for H and CO atoms. Preferred and minor desorption pathways are displayed in orange and blue, respectively. In (B) the preferred pathway for H_2 desorption is via the Pd site. In (C) the Pd site is blocked by CO, so H atoms spillover to Au and then desorb from there. All energies are reported relative to H_2 in the gas phase, as noted by the dashed horizontal lines.

Combining our TPD results with DFT calculations (Table S1-S3), we have elucidated the potential energy landscape for H_2 activation, diffusion and desorption from Pd-Au SAAs (Figure 4). The facile H_2 activation and weak adsorption of H atoms observed for Pd-Au SAAs are very different from those on monometallic Pd and Au surfaces (Figure 4A). On Au(111), H_2 activation and H adsorption is kinetically and thermodynamically unfavorable, respectively.[5,43,58] In order for H_2 from the gas phase to adsorb onto Au(111), it must overcome a large activation barrier, E_a which we calculate to be 1.04 eV, in agreement with other DFT calculations[5,58]

Additionally, H adsorption on fcc sites of Au(111) is thermodynamically unfavorable with respect to gas phase H_2 by 0.14 eV, within the current computational set-up. H_2 adsorption onto Pd(111), however, is a non-activated process which is barrier-less, with the resulting H atoms adsorbing strongly at fcc sites of Pd(111) with an adsorption energy of -0.58 eV per H adatom. With Pd-Au SAAs, we observed facile H_2 activation compared to Au and low temperature desorption of H_2 compared to Pd. For dilute concentrations of Pd in Au, we report H_2 dissociation at 85 K indicating that Pd monomers greatly reduce the activation barrier for the dissociation of H_2 compared to Au(111). Our DFT calculations support a reduction in the activation energy, since the transition state energy for H_2 on Pd-Au SAA is 0.20 eV compared to 1.04 eV for Au(111). Yet, the calculated transition state energies do not account for quantum nuclear effects which are likely to lead to make hydrogen adsorption more facile. Indeed previously, we have shown with path-integral based DFT simulations for atomic and molecular hydrogen that because of quantum mechanical tunneling, the effective free energy barrier for adsorption/desorption can be lowered. After dissociation, H binds to a Pd-Au fcc site with a computed adsorption energy of -0.11 eV. The negative adsorption energies correspond to exothermic adsorption processes, which are significantly weaker than when H binds to pristine Pd(111) (-0.58 eV) (Figure 4). The smaller adsorption energy of H to Pd-Au sites compared to Pd(111) occurs mainly because H binds in 3-fold hollow sites composed of 1 Pd atom and 2 Au atoms.[32,59] In order to adhere to microscopic reversibility, the adsorption and desorption of H_2 must follow the lowest energy pathway which is via the isolated Pd atoms in Au. The total desorption barrier is dependent on the H_2 activation energy and H adsorption energy which is directly related to the observed desorption temperatures. In order for H_2 to desorb from Pd-Au SAA, H atoms overcome both the weak adsorption energy of H to the Pd-Au sites and the

reduced H_2 activation barrier of Pd monomers (Figure 4B). Due to the thermodynamic instability of H atoms on Au, H atoms adsorb preferentially at Pd-Au sites, but a small quantity of H atoms exist on Au due to spillover from Pd-Au sites. The H atoms that exist on Au desorb directly from Au(111) with a desorption barrier of 1.04 eV. Though the overall desorption barrier of H_2 from Au is less than the desorption barrier from Pd-Au sites, H_2 predominately desorbs from Pd-Au sites due to the low surface coverage of H on Au.

When we consider the co-adsorption of H and CO we find that the desorption pathway of H_2 from the alloyed surface is altered (Figure 4C). Our DFT calculations reveal a greater thermodynamic stability for CO to occupy Pd-Au sites instead of H atoms. The adsorption of CO (-1.34 eV) on Pd monomers is significantly stronger than the adsorption of H to Pd monomers (-0.11 eV). Therefore, when a H covered Pd-Au surface is exposed to CO at 85 K, the H atoms are forced from the Pd-Au to Au sites. Although it is thermodynamically unfavorable for H to adsorb on pure Au, the H_2 recombination barrier traps it there until 110 K at which point H_2 desorbs from Au sites. CO changes the exit sites for H_2 from Pd atoms to Au sites without violating microscopic reversibility since the addition of CO makes the forward and reverse pathways non-equivalent. Interestingly, CO can force H atoms to spill over from a preferred site to a thermodynamically unstable site and remain trapped on the surface by the recombination barrier.

By utilizing well-defined Pd-Au model surfaces, we experimentally demonstrate that Pd monomers in a Au(111) surface can activate H_2, a process suggested by other experiments to require two contiguous Pd atoms. We clearly show by coupling high resolution STM with TPD, low concentrations of individual, isolated Pd atoms can dissociate H_2 since the concentration of adsorbed H atoms is proportional to the surface concentration of Pd atoms in Au. Combining

TPD with DFT calculations, we elucidate the energetic landscape for H_2 adsorption, activation, and desorption from isolated Pd atoms revealing a low temperature pathway for H_2 activation and release through the Pd atoms with minimal spillover to Au. The co-adsorption of H_2 and D_2 leads to complete scrambling of H and D supporting the dissociation of H_2 and the transient existence of H atoms on Au. Additionally, Pd-Au SAAs bind CO significantly more weakly than Pd(111) (270 K vs. 450 K) which can potentially improve CO tolerance of the catalysts. The competitive adsorption of CO and H on the Pd- atoms force H atoms to spillover onto the Au surface altering the desorption pathway to an even lower temperature through Au.(110 K vs. 175 K). Our work demonstrates that individual, isolated Pd atoms in Au allow for facile H_2 activation and weak adsorption of H atoms, a key requirement for efficient and selective hydrogenation catalysis.

Acknowledgments

Research at Tufts University was supported by the Department of Energy (DOE FG02-10ER16170). Some of the research at UCL leading to these results received financial support from the European Research Council under the European Union's Seventh Framework Programme (FP/2007-2013)/ERC Grant Agreement No. 616121 (HeteroIce project) and the Royal Society through a Wolfson Research merit Award (A.M.). MD is funded by Engineering and Physical Sciences Research Council UK as part of a Doctoral Training Grant. The authors acknowledge the use of the UCL Legion High Performance Computing Facility (Legion@UCL), and associated support services, in the completion of the computational part of this work.

Supporting Information

Full description of the experimental methods and computational details including summary of calculated adsorption energies and configurations.

References

(1) Hagen, J. *Industrial Catalysis*, 2nd ed.; Wiley-VCH Verlag GMbH & Co: Weinheim, 2006.

(2) Ritter, J. A.; Ebner, A. D. State-of-the-Art Adsorption and Membrane Separation Processes for Hydrogen Production in the Chemical and Petrochemical Industries. *Sep. Sci. Technol.* **2007**, *42*, 1123–1193.

(3) Graetz, J. New Approaches to Hydrogen Storage. *Chem. Soc. Rev.* **2009**, *38*, 73–82.

(4) Nørskov, J. K.; Bligaard, T.; Logadottir, A.; Bahn, S.; Hansen, L. B.; Bollinger, M.; Bengaard, H.; Hammer, B.; Sljivancanin, Z.; Mavrikakis, M.; et al. Universality in Heterogeneous Catalysis. *J. Catal.* **2002**, *209*, 275–278.

(5) Hammer, B.; Nørskov, J. K. Why Gold Is the Noblest of All the Metals. *Nature* **1995**, *376*, 238–240.

(6) Greeley, J.; Mavrikakis, M. Alloy Catalysts Designed from First Principles. *Nat. Mater.* **2004**, *3*, 810–815.

(7) Fu, Q.; Luo, Y. Catalytic Activity of Single Transition-Metal Atom Doped in Cu(111) Surface for Heterogeneous Hydrogenation. *J. Phys. Chem. C.* **2013**, *117*, 14618–14624.

(8) Skoplyak, O.; Barteau, M. A.; Chen, J. G. Reforming of Oxygenates for H_2 Production: Correlating Reactivity of Ethylene Glycol and Ethanol on Pt(111) and Ni/Pt(111) with Surface D-Band Center. *J. Phys. Chem. B* **2006**, *110*, 1686–1694.

(9) Alayoglu, S.; Nilekar, A. U.; Mavrikakis, M.; Eichhorn, B. Ru-Pt Core-Shell Nanoparticles for Preferential Oxidation of Carbon Monoxide in Hydrogen. *Nat. Mater.* **2008**, *7*, 333–338.

(10) Kyriakou, G.; Boucher, M. B.; Jewell, A. D.; Lewis, E. A.; Lawton, T. J.; Baber, A. E.; Tierney, H. L.; Flytzani-Stephanopoulos, M.; Sykes, E. C. H. Isolated Metal Atom Geometries as a Strategy for Selective Heterogeneous Hydrogenations. *Science* **2012**, *335*, 1209–1212.

(11) Boucher, M. B.; Zugic, B.; Cladaras, G.; Kammert, J.; Marcinkowski, M. D.; Lawton, T. J.; Sykes, E. C. H.; Flytzani-Stephanopoulos, M. Single Atom Alloy Surface Analogs in $Pd_{0.18}Cu_{15}$ Nanoparticles for Selective Hydrogenation Reactions. *Phys. Chem. Chem. Phys.* **2013**, *15*, 12187–12196.

(12) Pei, G. X.; Liu, X. Y.; Wang, A.; Li, L.; Huang, Y.; Zhang, T.; Lee, J. W.; Jang, B. W. L.; Mou, C.-Y. Promotional Effect of Pd Single Atoms on Au Nanoparticles Supported on Silica for the Selective Hydrogenation of Acetylene in Excess Ethylene. *New. J. Chem.* **2014**, *38*, 2043–2051.

(13) Zhang, L.; Wang, A.; Miller, T.; Liu, X.; Yang, X.; Wang, W.; Li, L.; Huang, Y.; Mou, C.; Zhang, T. Efficient and Durable Au Alloyed Pd Single-Atom Catalyst for the Ullmann Reaction of Aryl Chlorides in Water. *ACS Catal.* **2014**, *4*, 1546–1553.

(14) Cao, X.; Ji, Y.; Luo, Y. Dehydrogenation of Propane to Propylene by a Pd/Cu Single-Atom Catalyst: Insight from First-Principles Calculations. *J. Phys. Chem. C* **2015**, *119*, 1016–1023.

(15) Claus, P. Heterogeneously Catalysed Hydrogenation Using Gold Catalysts. *Appl. Catal.* **2005**, *291*, 222–229.

(16) Mcewan, L.; Julius, M.; Roberts, S.; Fletcher, J. C. Q. A Review of the Use of Gold Catalysts in Selective Hydrogenation Reactions. *Gold Bull.* **2010**, *43*, 298–306.

(17) Haruta, M. Size- and Support-Dependency in the Catalysis of Gold. *Catal. Today* **1997**, *861*, 153–166.

(18) Mohr, C.; Hofmeister, H.; Radnik, J.; Claus, P. Identification of Active Sites in Gold-Catalyzed Hydrogenation of Acrolein. *J. Am. Chem. Soc.* **2003**, *103*, 178–180.

(19) Chen, M.; Kumar, D.; Yi, C.-W.; Goodman, D. W. The Promotional Effect of Gold in Catalysis by Palladium-Gold. *Science* **2005**, *310* (5746), 291–293.

(20) Edwards, J. K.; Solsona, B.; Ntainjua N, E.; Carley, A. F.; Herzing, A. A.; Kiely, C. J.; Hutchings, G. J. Switching off Hydrogen Peroxide Hydrogenation in the Direct Synthesis Process. *Science* **2009**, *323*, 1037–1041.

(21) Choudhary, T. V; Sivadinarayana, C.; Datye, A. K.; Kumar, D.; Goodman, D. W. Acetylene Hydrogenation on Au-Based Catalysts. *Catal. Letters* **2003**, *86*, 1–8.

(22) Hugon, A.; Delannoy, L.; Krafft, J. M.; Louis, C. Selective Hydrogenation of 1,3-Butadiene in the Presence of an Excess of Alkenes over Supported Bimetallic Gold−palladium Catalysts. *J. Phys. Chem. C.* **2010**, *114*, 10823–10835.

(23) Gao, F.; Wang, Y.; Goodman, D. W. CO Oxidation over AuPd(100) from Ultrahigh Vacuum to near-Atmospheric Pressures: The Critical Role of Contiguous Pd Atoms. *J. Am. Chem. Soc.* **2009**, *131*, 5734–5735.

(24) Enache, D. I.; Edwards, J. K.; Landon, P.; Solsona-Espriu, B.; Carley, A. F.; Herzing, A. a; Watanabe, M.; Kiely, C. J.; Knight, D. W.; Hutchings, G. J. Solvent-Free Oxidation of Primary Alcohols to Aldehydes Using Au-Pd/TiO_2 Catalysts. *Science* **2006**, *311*, 362–365.

(25) Rodriguez, J. A.; Rodriguex, J. A. Physical and Chemical Properties of Bimetallic Surfaces. *Surf. Sci. Rep.* **1996**, *24*, 223–287.

(26) Groß, A. Reactivity of Bimetallic Systems Studied from First Principles. *Top. Catal.* **2006**, *37*, 29–39.

(27) Neurock, M.; Tysoe, W. T. Mechanistic Insights in the Catalytic Synthesis of Vinyl Ccetate on Palladium and Gold/palladium Alloy Surfaces. *Top. Catal.* **2013**, *56*, 1314–1332.

(28) Yu, W.-Y.; Mullen, G. M.; Mullins, C. B. Hydrogen Adsorption and Absorption with Pd-Au Bimetallic Surfaces. *J. Phys. Chem. C* **2013**, *117*, 19535–19543.

(29) Maroun, F.; Ozanam, F.; Magnussen, O. M.; Behm, R. J. The Role of Atomic Ensembles in the Reactivity of Bimetallic Electrocatalysts. *Science* **2001**, *293*, 1811–1814.

(30) Venkatachalam, S.; Jacob, T. Hydrogen Adsorption on Pd-Containing Au(111) Bimetallic Surfaces. *PCCP* **2009**, *11* (17), 3010.

(31) Baber, A. E.; Tierney, H. L.; Sykes, E. C. H. Atomic-Scale Geometry and Electronic Structure of Catalytically Important Pd/Au Alloys. *ACS Nano.* **2010**, *4*, 1637–1645.

(32) Ruff, M.; Takehiro, N.; Liu, P.; Nørskov, J. K.; Behm, R. J. Size-Specific Chemistry on Bimetallic Surfaces: A Combined Experimental and Theoretical Study. *ChemPhysChem* **2007**, *8*, 2068–2071.

(33) Casari, C.; Foglio, S.; Siviero, F.; Li Bassi, A.; Passoni, M.; Bottani, C. Direct Observation of the Basic Mechanisms of Pd Island Nucleation on Au(111). *Phys. Rev. B* **2009**, *79*, 1–9.

(34) Barth, J. V.; Brune, H.; Ertl, G.; Behm, R. J. Scanning Tunneling Microscopy Observations on the Reconstructed Au(111) Surface: Atomic Structure, Long-Range Superstructure, Rotational Domains, and Surface Defects. *Phys. Rev. B* **1990**, *42*, 9307–9318.

(35) Meyer, J. A.; Baikie, I. D.; Kopatzki, E.; Behm, R. J. Preferential Island Nucleation at the Elbows of the Au(111) Herringbone Reconstruction through Place Exchange. *Surf. Sci.* **1996**, *365*, 647–651.

(36) Yudanov, I. V; Neyman, K. M. Stabilization of Au at Edges of Bimetallic PdAu Nanocrystallites. *Phys. Chem. Chem. Phys.* **2010**, *12*, 5094–5100.

(37) Yuan, D.; Gong, X.; Wu, R. Atomic Configurations of Pd Atoms in PdAu(111) Bimetallic Surfaces Investigated Using the First-Principles Pseudopotential Plane Wave Approach. *Phys. Rev. B* **2007**, *75*, 085428–1 – 5.

(38) Sugimoto, T.; Fukutani, K. Effects of Rotational-Symmetry Breaking on Physisorption of Ortho- and Para- H_2 on Ag(111). *Phys. Rev. Lett.* **2014**, *112*, 146101–1 – 5.

(39) Andersson, S.; Persson, M. Crystal-Face Dependence of Physisorption Potentials. *Phys. Rev. B* **1993**, *48*, 5685–5688.

(40) Gdowski, G. E.; Felter, T. E.; Stulen, R. H. Effect of Surface Temperature on the Sorption of Hydrogen on Pd(111). *Surf. Sci.* **1987**, *181*, L147–L155.

(41) Pan, M.; Flaherty, D. W.; Mullins, C. B. Low-Temperature Hydrogenation of Acetaldehyde to Ethanol on H-Precovered Au(111). *J. Phys. Chem. Lett.* **2011**, *2*, 1363–1367.

(42) Baber, A. E.; Tierney, H. L.; Lawton, T. J.; Sykes, E. C. H. An Atomic-Scale View of Palladium Alloys and Their Ability to Dissociate Molecular Hydrogen. *Chem. Cat. Chem* **2011**, *3*, 607–614.

(43) Tierney, H. L.; Baber, A. E.; Kitchin, J. R.; Sykes, E. C. H. Hydrogen Dissociation and Spillover on Individual Isolated Palladium Atoms. *Phys. Rev. Lett.* **2009**, *103*, 246102–1 – 4.

(44) Pan, M.; Pozun, Z. D.; Yu, W.-Y.; Henkelman, G.; Mullins, C. B. Structure Revealing H/D Exchange with Co-Adsorbed Hydrogen and Water on Gold. *J. Phys. Chem. Lett.* **2012**, *3*, 1894–1899.

(45) Guo, X.; Yates, J. T. Dependence of Effective Desorption Kinetic Parameters on Surface Coverage and Adsorption Temperature: CO on Pd(111). *J. Chem. Phys.* **1989**, *90*, 6761–6766.

(46) Kim, J.; Samano, E.; Koel, B. E. CO Adsorption and Reaction on Clean and Oxygen-Covered Au(211) Surfaces. *J. Phys. Chem. B* **2006**, *110*, 17512–17517.

(47) Yi, C.-W.; Luo, K.; Wei, T.; Goodman, D. W. The Composition and Structure of Pd-Au Surfaces. *J. Phys. Chem. B* **2005**, *109*, 18535–18540.

(48) Kresse, G.; Furthmüller, J. Efficiency of Ab-Initio Total Energy Calculations for Metals and Semiconductors Using a Plane-Wave Basis Set. *Comput. Mater. Sci.* **1996**, *6*, 15–50.

(49) Kresse, G.; Furthmuller, J. Efficient Iterative Schemes for Ab Initio Total-Energy Calculations Using a Plane-Wave Basis Set. *Phys. Rev. B* **1996**, *54* (16), 11169–11186.

(50) Klimes, J.; Bowler, D. R.; Michaelides, A. Chemical Accuracy for the Van Der Waals Density Functional. *J. Phys. Condens. Matter* **2010**, *22* (2), 22201.

(51) Klimes, J.; Bowler, D. R.; Michaelides, A. Van Der Waals Density Functionals Applied to Solids. *Phys. Rev. B* **2011**, *83* (19), 195131.

(52) Dion, M.; Rydberg, H.; Schroder, E.; Langreth, D. C.; Lundqvist, B. I. Van Der Waals Density Functional for General Geometries. *Phys. Rev. Lett.* **2004**, *92* (24), 246401.

(53) Rupprechter, G.; Morkel, M.; Freund, H.-J.; Hirschl, R. Sum Frequency Generation and Density Functional Studies of CO–H Interaction and Hydrogen Bulk Dissolution on Pd(111). *Surf. Sci.* **2004**, *554*, 43–59.

(54) Ogura, S.; Okada, M.; Fukutani, K. Near-Surface Accumulation of Hydrogen and CO Blocking Effects on a Pd − Au Alloy. *J. Phys. Chem. C* **2013**, *117*, 9366–9371.

(55) Marcinkowski, M. D.; Jewell, A. D.; Stamatakis, M.; Boucher, M. B.; Lewis, E. A.; Murphy, C. J.; Kyriakou, G.; Sykes, E. C. H. Controlling a Spillover Pathway with the Molecular Cork Effect. *Nat. Mater.* **2013**, *12*, 523–528.

(56) Lewis, E. A.; Le, D.; Jewell, A. D.; Murphy, C. J.; Rahman, T. S.; Sykes, E. C. H. Visualization of Compression and Spillover in a Coadsorbed System: Syngas on Cobalt Nanoparticles. *ACS Nano* **2013**, *7*, 4384–4392.

(57) Lewis, E. a.; Marcinkowski, M. D.; Murphy, C. J.; Liriano, M. L.; Sykes, E. C. H. Hydrogen Dissociation, Spillover, and Desorption from Cu-Supported Co Nanoparticles. *J. Phys. Chem. Lett.* **2014**, *5*, 3380–3385.

(58) Campbell, C. T. Bimetallic Surface Chemistry. *Annu. Rev. Phys. Chem.* **1990**, *41*, 775–837.

(59) Boscoboinik, J. a.; Calaza, F. C.; Garvey, M. T.; Tysoe, W. T. Identification of Adsorption Ensembles on Bimetallic Alloys. *J. Phys. Chem. C* **2010**, *114*, 1875–1880.